

## Selection of the method for determination of ignition delay of hypergolic propellants

### ARTICLE INFO

Received: 5 July 2024  
Revised: 23 July 2024  
Accepted: 18 August 2024  
Available online: 20 August 2024

*Ignition delay is one of the most important parameters characterising hypergolic propellants. This parameter has a strong impact on thruster operation, especially during the cold start. Ignition delay influences the intensity of pressure rise and its peak values during the start of a thruster. High-pressure levels cause stress inside the chamber wall, which directly affects durability and safety. One of two measurement techniques is usually chosen to determine the ignition delay: visual and pressure-based methods. Visual methods are based on high-speed imaging and subsequent image analysis. In the pressure-based method, the pressure trace is analysed. In this study, both techniques were used together and compared in terms of ignition delay determination of hypergolic propellants igniting during the drop tests. The advantages and disadvantages of both techniques were indicated and described. In the setup used in the study, the visual method was found to be more accurate and reliable.*

**Key words:** *ignition delay, hypergolic ignition, hypergolic propellants, drop test*

This is an open access article under the CC BY license (<http://creativecommons.org/licenses/by/4.0/>)

### 1. Introduction

The ignition delay of hypergolic propellants is usually determined by a so-called drop-test method where a drop of oxidiser (or fuel) is dropped into the fuel (or oxidiser) pool [1–5, 7–9, 12, 18, 19, 23–25, 33, 34, 37–39]. In such an arrangement, the ignition delay is determined as the time between the contact of the oxidiser with the fuel and the start of combustion (SOC). In this study, we focus on the determination of SOC.

Alfano et al. [2] used a high-speed camera, two photodiodes and a laser diode to determine the ignition delay and chemical delay in the drop tests. Based on the registered signals, they identified the moment of droplet impact, gas emission near the surface, and light emission from combustion.

Blevins et al. [3] used high-speed photography and Schlieren techniques to determine hypergolic ignition delay between hydrogen peroxide (an oxidiser) and N,N-dimethylbutylamine and N,N-dimethylhexylamine (fuels). The amines were mixed with a catalyst (cobalt II 2-ethylhexanoate) and mineral oil, acting as a stabiliser (prepared as mixtures in a 65% to 35% ratio). The catalyst and stabiliser constituted 5% of the final fuel mixture. The Schlieren imaging enabled the visualisation of enhanced gas-phase generation, which was associated with the decomposition time. Thus, the reported results included both decomposition delay and ignition delay.

Another work utilising the drop test method to measure ignition time delay was conducted by Kang et al. [20]. They tested the ignition of three different fuels with hydrogen peroxide (90%, 95%, and 98%) acting as oxidiser. To measure the ignition delay, they used a high-speed camera with an additional halogen lamp to illuminate falling droplets. Mahakali et al. [24] also used the drop-test method with a high-speed camera to determine the existence of ignition and ignition delay for a group of fuels (triglyme, dimethyl formamide, and dimethyl sulfoxide) with the addition of sodium borohydride (in various concentrations).

They used hydrogen peroxide with a concentration between 87.4% and 88.5% as the oxidiser.

McCrary et al. [25] employed the drop test technique with a high-speed camera to measure the ignition delay of synthesised fuels with various oxidisers (99.5% white fuming nitric acid (WFNA), inhibited red fuming nitric acid (IRFNA), and 70% nitric acid (NA)). In their setup, the oxidiser drops were dropped onto samples of the fuels. Ramachandran et al. [34] used the drop test technique to measure ignition time delay for WFNA and amine-borane with a high-speed camera and an LED light array to illuminate the fuel sample and the oxidiser.

Wang and Thynell [37] used a similar method to measure the ignition delay of MMH with three different mixtures of nitric acid and water (30% H<sub>2</sub>O, 10% H<sub>2</sub>O, and WFNA). However, they also measured signals from thermocouples (located at two distances from the fuel pool), photodiodes, and a microphone. They compared the measurements from the photodiode with the signal from the microphone and thermocouples. The signals correlated differently depending on the propellant type, exhibiting sensitivity to the fuel-oxidiser interaction type.

Zarbo et al. [38] studied the effect of humidity and water on the reaction between two pairs of fuel and oxidiser: MMH-RFNA and TEAB (triethylamine borane)-WFNA. The measurements were conducted in a dedicated and developed drop-test stand using a high-speed camera, a piezoelectric sensor to detect droplet impact, and a photodiode to detect the onset of ignition. Zhan and Shreeve [39] also used the drop-test method with a high-speed camera to determine the ignition delay of nine fuels (with three boron-based additives) with WFNA.

Ak et al. [1] used a high-speed camera to measure the ignition delay for 85% hydrogen peroxide and ethanalamine in open-cup drop-test experiments. They assessed the influence of oxidiser and fuel temperature on the ignition time delay. Chambreau et al. [4] applied Fourier-transform

infrared (FTIR) absorption spectroscopy using a rapid-scan spectrometer to observe drop-test experiments for 1-propargyl-3-methyl-imidazolium dicyanamide or MMH with WFNA or RFNA. Chowdhury et al. [5] used the drop test with high-speed photography to observe photodiode signal and laser-induced fluorescence to study the mixing between the liquids. In the drop tests, they used two fuels: 1-ethyl-3-methyl-imidazolium dicyanamide and 1-butyl-3-methyl-imidazolium dicyanamide, reacting with 70% and 90% WFNA.

Coil [7] used the drop test to study the ignition of gelled methyl ethyl imidazolium dicyanamide (fuel) with nitric acid (oxidiser). They applied high-speed photography and a photoresistor to determine the ignition delay. Dambach et al. [8] used the drop-test technique with a high-speed camera to observe the ignition process of several selected fuels with RFNA and determine ignition delay. Davis and Yilmaz [9] used a high-speed camera and photodiode to observe the ignition delay of hydrazine and hydrogen peroxide in the drop tests.

Jyoti et al. [18] used the drop-test method with a high-speed camera to measure the ignition delay of gelled ethanol and 90% hydrogen peroxide. Kang et al. [20] also employed the drop test with a high-speed camera for a preliminary approximation of the ignition time delay of a developed fuel with 95% and 98% hydrogen peroxide. Zhao et al. [40] used a high-speed camera in a drop test to observe the ignition and combustion process of specially prepared compounds with  $\text{HNO}_3$ .

Park et al. [31] utilised a drop-test technique with a laser, photodiode, and fast camera to observe the ignition delay of 95% hydrogen peroxide with  $\text{LiNO}_3$  and  $\text{NH}_4\text{NO}_3$ . In their tests, the fuels contained different amounts of water (0.5%, 1.0%, 5.0%, and 20%). Several high-speed cameras (infrared, monochrome, and colour) and sensors with a laser and LED lamp were used by Nath et al. [30] in drop tests of hydrogen peroxide and high-density polyethylene mixed with  $\text{NaBH}_4$ . Mota et al. [27] used three high-speed cameras operating in visible, schlieren, and infrared spectra (IR) modes to observe the ignition delay in drop tests of several selected fuels with hydrogen peroxide. Khomik et al. [22] also employed a high-speed camera to observe the ignition time delay in open-cup drop tests.

Pourpoint and Anderson [33] tested the ignition delay of catalytically promoted fuels with highly concentrated hydrogen peroxide (92% to 98%) using an impinging jet apparatus with a high-speed camera. James et al. [16] also used a high-speed camera to observe the ignition delay in impinging-jets tests with gelled hypergolic propellants. Similarly, DeSain et al. [10] used a fast camera to determine the ignition time delay in their experiments. He et al. [14] also employed a high-speed camera to observe the ignition of gelled hydrogen peroxide with various fuels.

As far as ignition delay studies are concerned, there are two main methods that are usually used for the determination of the start of combustion: visual [3, 5, 8, 9, 12, 16, 18, 19, 23, 24] and pressure-based [11, 15, 29, 32]. Visual observation has one strong advantage – one recording can be used for both the determination of the time of contact between an oxidiser and a fuel and the start of combustion

[1, 25, 33, 34, 37, 39]. With a known frame rate and a number of frames between these two detected incidents, ignition delay can be calculated. The second method is based on data analysis from a pressure sensor. The pressure inside the chamber increases during combustion in a constant volume chamber. The time, which represents the beginning of combustion, may be defined by the intersection of two lines. The first line represents the average pressure before combustion, while the second is tangent to the pressure curve at its maximum slope. For the detection of the instant contact (between the oxidiser and the fuel), we used high-speed cameras. However, some researchers use photodiodes [9].

The presented literature shows that, in the drop tests, the optical methods are preferred. However, most studies on hypergolic ignition were performed in an open environment. The pressure-based method, in turn, is only applicable in enclosed-volume research devices, such as constant-volume chambers [17, 29], rapid-compression machines [26], or shock tubes [11, 15]. Both of these techniques could be applied in this study, as the drop tests were performed in a constant volume vessel. It should be noted that other methods for estimating ignition delay also exist. Szwaja and Szymanek [35] also used registered pressure trace, but indirectly. First, they calculated heat release, which was then used to determine ignition delay. Chwist [6], in turn, used ANSYS Chemkin Pro for this purpose, which numerically calculates ignition delay.

The goal of the study was to assess and compare both methods in terms of determining the ignition delay of hypergolic propellants by the drop-test method. The data from the pressure sensor and high-speed camera images were taken simultaneously. Thus, both methods were used to determine ignition delay for the same cases, and a direct comparison of these two methods could be made.

For this verification, prospective “green” propellant was chosen, as these kinds of fuels and oxidisers have received much attention recently [28, 36]. Pyridine (with the addition of a catalyst) was used as a fuel, while the HTP (high-test peroxide, also named RGHP – rocket grade hydrogen peroxide [9]) was selected as an oxidiser.

As discussed earlier, most researchers conducted their experiments in an open environment, which means that the reported results were limited to atmospheric conditions [5, 8, 10, 16, 18, 20, 23, 24]. Only a small part of studies have investigated the effect of pressure and temperature on ignition delay [9, 10, 33]. The verification tests presented here were performed for different environmental pressures (0.1, 1, and 2 MPa absolute pressure) and fuel temperatures (295 and 353 K) to make our comparison more universal. In all tests, the oxidiser temperature was 293 K (in a syringe). Ak et al. [1] performed experiments that showed low dependence on ignition delay from oxidiser temperature and high dependence on fuel temperature.

## 2. Materials and methodology

### 2.1. Experimental setup

The research was performed using a specially modified constant-volume chamber initially designed for spray tests of marine engine injectors [13]. The chamber was adapted for the drop-test method by providing an oxidiser dosing

unit (Fig. 1) and a fuel pool with a temperature control (Fig. 2). The chamber was pressurised with air. The droplet release and the ignition process were observed through the quartz window by the high-speed camera. The test chamber was also equipped with fast-access entry, which allowed us to refill the fuel after each test.

The dosing system was composed of a high-pressure syringe, a holder for the syringe, which also holds a linear module with a stepper motor (Fig. 1). The stepper motor drives the linear module coupled with the syringe. The holder was designed to eliminate vibrations generated by the stepper motor.

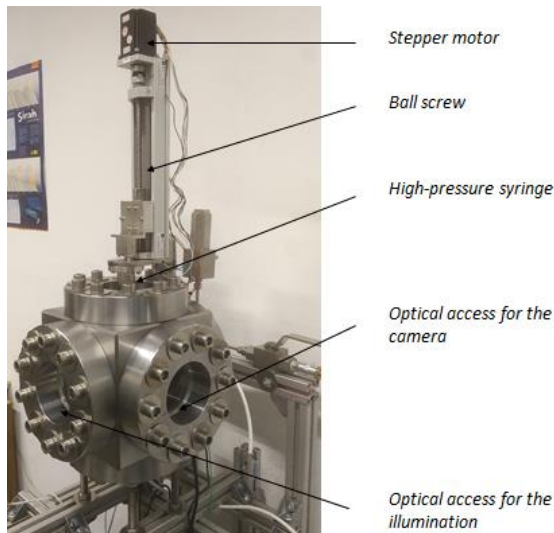


Fig. 1. Modified constant volume chamber for drop-test studies

The vessel was also equipped with a pressurised gas delivery system, an electric heater, and a thermocouple with a temperature controller. The thermocouple was placed one millimetre under the bottom of the fuel pool.

Two holes in the chamber were filled by quartz windows. One window was used to illuminate falling droplets, while the second one provided optical access for a high-speed camera. The fuel pool was made of stainless steel, and it was thermally insulated from the bottom of the chamber. The electric band heater was wrapped around the fuel pool (Fig. 2).

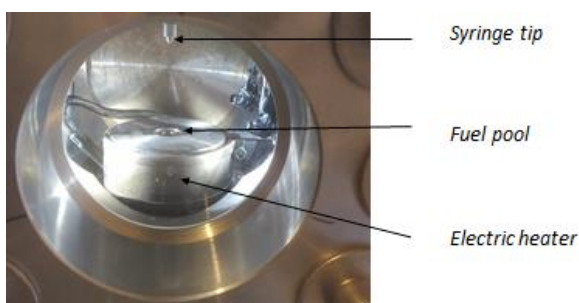


Fig. 2. Fuel pool with a heater for temperature control

The pressure inside the chamber was measured by a piezoelectric pressure transducer (KISTLER 601CA). The pressure and temperature signals were recorded by a data acquisition system (DEWETRON DEWE-50-PCI-16). The

pressure signal was recorded at a frequency of 10 kHz. The pressure transducer, charge signal converter and amplifier were configured to measure pressure within the range of 0-5 MPa (absolute). The data acquisition started 1 second before the trigger signal and ended 0.5 seconds after that signal. The trigger signal was generated based on the pressure measurement – when the pressure increase was higher than two kilopascals (above the environmental pressure) for at least three milliseconds.

High-speed camera (Photron SA 1.1) operated at a frame rate of 10 kHz. This frame rate allowed us to determine the moment of self-ignition with an accuracy of 0.1 ms. In order to capture contact of a drop with a pool and the start of combustion, the camera was set to continuous recording and storage mode (operating in a loop limited by the camera memory). The trigger signal was set at the end of the recording. These settings enabled the recording of more than 1 second, which was enough to capture both the moment of contact of the fuel with the oxidiser and the start of combustion.

## 2.2. Visual analysis

Based on the recorded images, the time of contact between the oxidiser droplet and the fuel, as well as the moment of occurrence of visible effects of the combustion process (identified here as the start of combustion), were determined. Two effects of combustion could be noticed, i.e., increased emission of visible light (Fig. 3) or fast increasing expansion of gases, which caused braking of the fuel surface (Fig. 4).

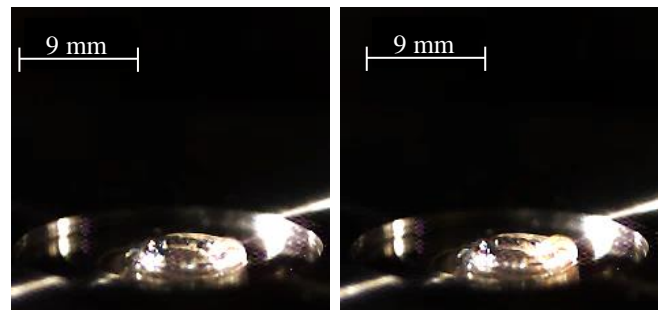


Fig. 3. Beginning of combustion with light emission (two consecutive frames)

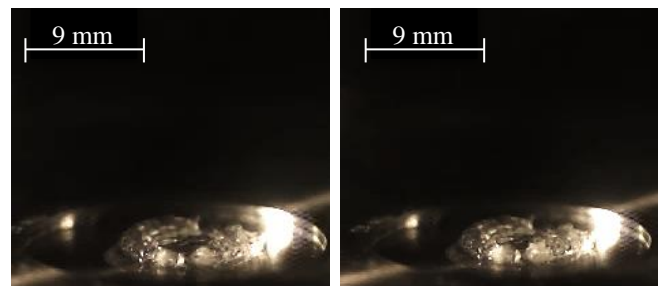


Fig. 4. Beginning of combustion with a brake of the liquid surface caused by decomposition or combustion gases (two consecutive frames)

With determined time of contact and SOC as well as known frame rate, the ignition delay (ID) was calculated according to the equation (1):

$$ID = \frac{n_{ign} - n_{con}}{f} \quad (1)$$

where:  $n_{ign}$  – number of the frame with the identified start of the combustion;  $n_{con}$  – number of the frame with the identified beginning of contact between the oxidiser drop and the fuel pool;  $f$  – frame rate.

### 2.3. Pressure-trace analysis

In the pressure-based method, SOC is determined based on the analysis of the recorded pressure curve. For this purpose, two lines need to be drawn. The first line corresponds to the average pressure level before combustion. The second one is tangent to the pressure curve at its maximum slope, associated with the fastest pressure increase due to the combustion process. The time at the intersection of these two lines is defined as the start of combustion (Fig. 5).

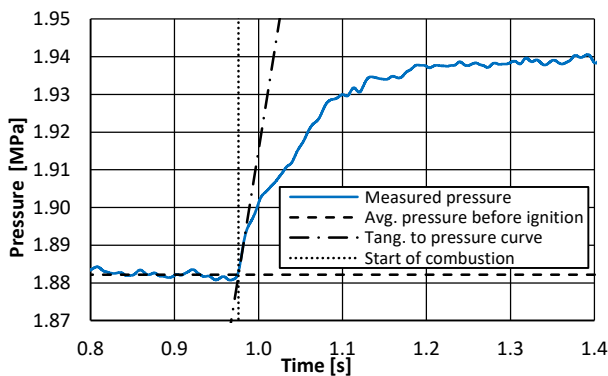


Fig. 5. Example pressure trace in the chamber, with a cross of two lines to determine the start of combustion; time measured from the start of the data acquisition

Note that the time reported in Fig. 5 was measured from the start of the data acquisition. To calculate the ignition delay, the time of contact between the oxidiser and the fuel needs to be determined as well. However, based on pressure trace analysis, it is impossible to determine the moment of contact between oxidiser and fuel. It is necessary to use high-speed imaging anyway. These two measurement methods need to be used together and synchronised in order to combine the data obtained by them. With a known start of combustion and a time of contact of the oxidiser with the fuel, the ignition delay can be determined.

### 2.4. Measurement procedure

The measurement procedure included the following steps:

1. Setting the temperature of the pool (temperature was measured by type J thermocouple placed 1 mm below the bottom of fuel pool)
2. Opening and cleaning the chamber and windows
3. Filling up the syringe with HTP (if needed)
4. Filling the pool with the fuel
5. Closing and pressurising the chamber
6. Setting up data acquisition and trigger mode
7. Moving the syringe piston for dropping a drop of the oxidiser
8. Saving data (camera recording, pressure data)
9. Scavenging the chamber and releasing the combustion gases into the exhaust-extraction duct.

Steps 2–9 were repeated seven times for each measurement point.

## 3. Results

### 3.1. High-speed imaging

Based on recorded images for pyridine and HTP, the ignition delay was calculated. (as described in chapter 2.2). Figure 6 shows the determined ignition delay obtained at three different environmental pressures and for two different fuel temperatures.

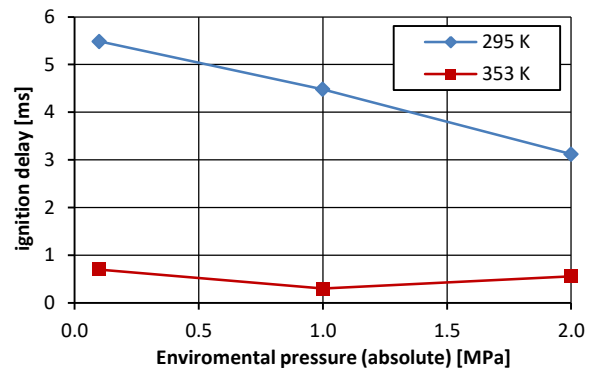


Fig. 6. Ignition delay; calculated using SOC determined by high speed-imaging for two different fuel temperatures

### 3.2. Pressure-based SOC determination

The ignition delay was also determined using recorded pressure data for the same cases. In this procedure, the ignition delay was calculated by combining two methods. The moment of contact of the oxidiser droplet and fuel in the pool was determined by the high-speed camera, while the SOC was determined based on pressure recording (as described in section 2.2). The results of the calculations for two different fuel temperatures are presented in Fig. 7.

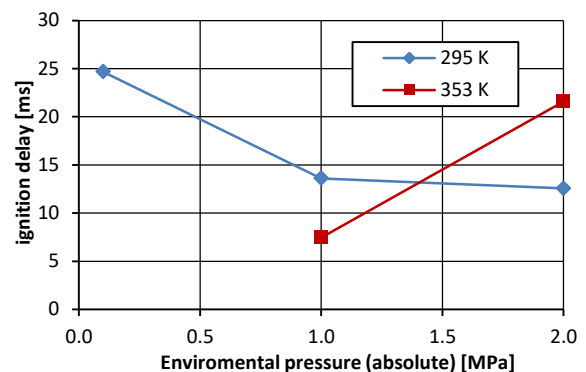


Fig. 7. Ignition delay versus absolute pressure for two different fuel temperatures (SOC determined by pressure-based method)

In the current setup used for drop-test studies, the mass of the fuel was small compared to the volume of the chamber (and thus the mass of the enclosed air). Moreover, energy initially released in one point of the chamber (at the droplet impact point) couldn't rapidly increase temperature and pressure. The whole fuel needed to be consumed until the pressure change was high enough to distinguish it from the noise signal. Thus, the values presented in Fig. 7 are



much higher than those obtained with the visual method (see Fig. 6).

#### 4. Discussion

This section aims to discuss the advantages and disadvantages of the two techniques that were used.

With increasing temperature of the fuel pool, self-ignition delay decreases. This effect could be strengthened by the increasing concentration of catalytic additives in the fuel due to its intensive evaporation at high temperatures. The effect of fuel evaporation at high temperatures leading to an increased concentration of the catalytic additive (manifested by the white colour of the fuel pool) is shown in Fig. 8. The brighter colour of the droplet suggests that the temperature from the pool influenced the oxidiser as well, which supposedly started to decompose already during the free fall.

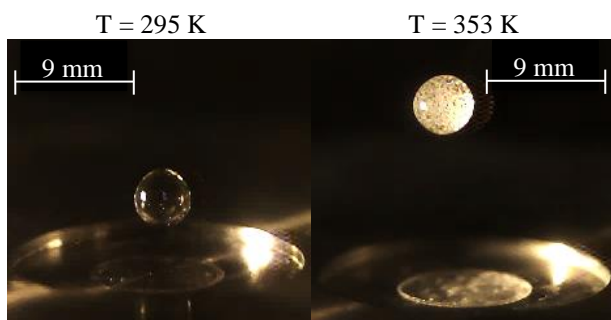


Fig. 8. Droplet of the oxidiser and the fuel pool for different fuel temperatures at 1 MPa absolute pressure

The fuel evaporation seemed to be decreased at increased pressure inside the chamber, which is presented in Fig. 9.

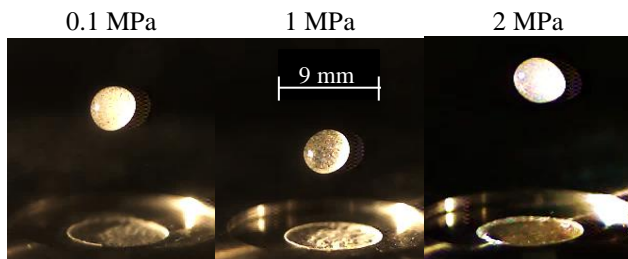


Fig. 9. Droplet of the oxidiser and the fuel pool at different pressures; fuel temperature 353 K

Regardless of these issues, other aspects could also be the reason for the poor repeatability of the results. One of them is the lack of temperature compensation in the pressure transducer. In some cases, droplets splashed from the pool and fell onto the sensor's surface, causing pressure curve breakdown (a sudden pressure drop). This effect is shown in Fig. 10. An additional issue during the estimation of SOC from the pressure curve is the shape of the recorded data. The recorded data was affected by a strong noise signal. Thus, the data from the piezoelectric transducer needed to be filtered. For this purpose, a simple moving average filtering algorithm with five symmetrical points was used. With repeating filtration cycles, filtered curves became smoother, but the large time-scale pressure changes were also affected. These were extended in time. The influence

of the number of filtrations on the pressure curve is presented in Fig. 11. Note that time is measured from the beginning of the recording.

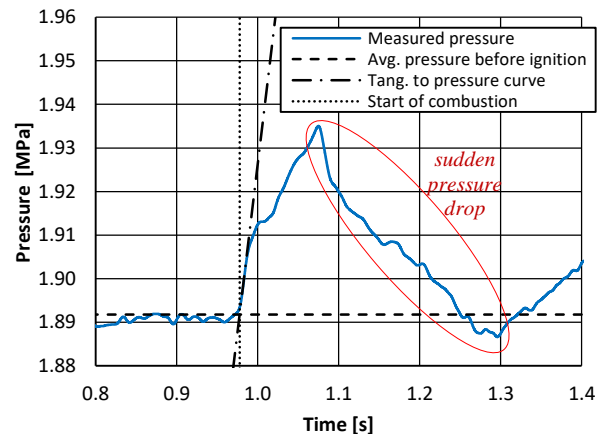


Fig. 10. Pressure curve breakdown caused by the droplet impact onto the sensor's surface

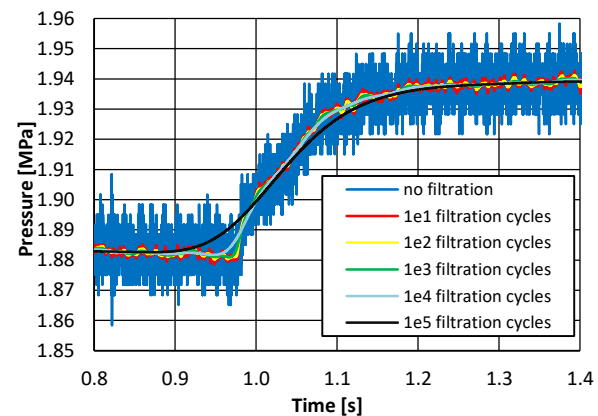


Fig. 11 Example pressure curve – raw data (no filtration) and filtered versions; time measured from the start of the data acquisition

Due to the effects of filtration on the large time-scale pressure features, the ignition delay was also affected. The ignition delay dependence on the number of filtration cycles is shown in Table 1.

Table 1. Ignition delay for different numbers of filtrations calculated from the same pressure curve

No. of filtrations	Ignition delay [ms]
0	18.9
10	46.6
100	51.4
1000	45.9
10000	34.7
100000	16.5
1000000	-80.7

Due to the strong noise signal determination of SOC for non-filtrated data, it is strongly problematic. Increasing the filtration number, in turn, advances the SOC. With an increasing number of filtration over  $10^2$ , the estimated ignition delay decreases even to nonphysical results, as in the case of  $10^6$  filtration. It might be speculated that the other type of filtration could perform better, and the issue of advancing the SOC could be avoided. However, the Butterworth filter used

in a similar setup also resulted in a delayed start of combustion compared to the visual ignition effects [21].

The other issue affecting the quality of pressure data, specifically the signal-to-noise ratio, was a decreasing combustion intensity with increasing fuel temperature. This was mainly caused by the evaporation of the fuel. This effect had a much lower influence on the optical method than on the pressure-based technique. An example pressure curve (environmental pressure: 1 MPa, fuel temperature 353 K) after 1000 cycles of filtrations is presented in Fig. 12. As one may observe, the shape of the curve is entirely different than that shown in Fig. 11 (environmental pressure: 2 MPa, fuel temperature: 333 K). In that case, the start of combustion could not be appropriately determined using the pressure data.

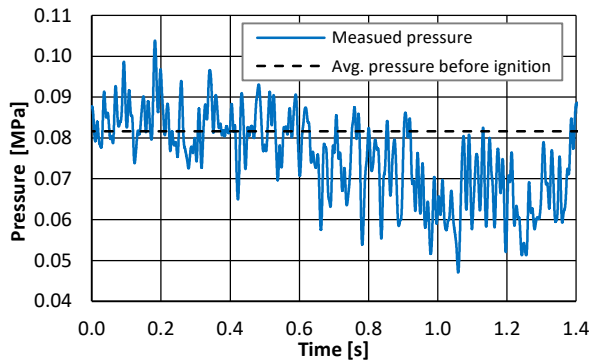


Fig. 12. Determination of SOC for 0.1 MPa absolute pressure and fuel temperature of 353 K

All presented reasons caused low repeatability of the results, especially those obtained using the pressure-based method to determine the start of combustion. The coefficient of variation for both methods is shown in Fig. 13.

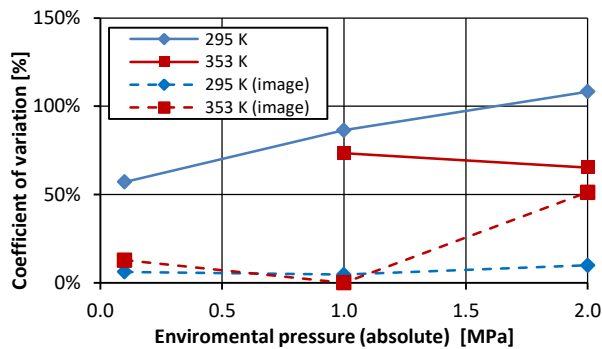
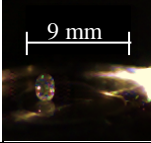



Fig. 13. Coefficient of variation of ignition delay for visual (dashed lines) and pressure-based methods (solid lines)

High-speed imaging-based ignition delay determination provided high repeatability of the results. The cases where the result deviated from the average could be associated with a specific aspect of the measurement, e.g. imprecise impingement point. Table 2. shows the cases when the droplet didn't impinge in the center of the fuel pool and reports the measured ignition delay. It also shows the average ignition delay (for seven repetitions) determined at the corresponding measurement point.

Table 2. Droplet impingement location and the corresponding ignition delay values

Parameters (fuel temperature and pressure in the chamber)	A photograph of droplet impingement	Measured ignition delay	Average ignition delay
T = 295 K p = 2 MPa		3.1 ms	2.2 ms
T = 333 K p = 1 MPa		2.2 ms	1.6 ms

An additional issue during the data analysis was related to the droplet oscillation. Figure 14 shows the evolution of the oscillating droplet prior to the impingement. The time displayed in each photograph represents the time remaining to the contact between the oxidiser and fuel.

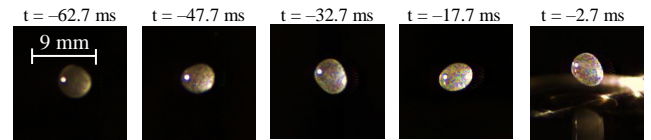


Fig. 14. Evolution of the oscillating droplet prior to the impingement

When using the visual method, the aspect of the oscillating droplet could be evaluated quantitatively by determining the droplet's geometrical features at the instant of the impingement, as was done in our previous study [21]. If the pressure method is applied, high-speed imaging would also be required.

In general, the repeatability of the results obtained using pressure-based SOC determination was much worse than that observed for visual SOC determination. Moreover, the ignition delay values obtained using the pressure-based method are much higher than those obtained by the optical method.

These observations suggest that the pressure-based technique is not acceptable for quantitative ignition delay measurement in the current setup.

### 5. Conclusions

Simultaneous image acquisition and pressure measurements enabled the direct comparison of two approaches for the start of combustion (and ignition delay) determination. Moreover, the study revealed other aspects which should be addressed when performing drop tests at high temperatures. The crucial aspect is that the delay between the fuel delivery and the test cannot be too long due to fuel evaporation and increasing concentration of the additive.

In terms of the start of combustion and ignition delay determination, the presented analysis allows us to conclude that the visual method is more reliable, accurate and better suited for the setup and propellants used in the study – mainly due to the relatively large volume of the test chamber (compared to the amount of fuel and the size of the fuel-oxidiser contact zone).

The advantages of this method were summarised as follows:

- high repeatability of measurement results
- no need for synchronisation of a high-speed camera with a pressure transducer
- easier evaluation of test quality (size and shape of the droplet, place of droplet impact, amount of fuel in the pool, etc.).

The main disadvantage of this technique is the need for a manually generated trigger signal, which could be overcome by using an additional photodiode triggering system.

The advantages of the pressure-based method are as follows:

- automatic trigger generation based on pressure
  - additional information on combustion process dynamics.
- In the setup used in the study, the pressure-based method had several disadvantages that make this method useless for ignition delay determination, especially when quantitative measurement is needed:
- high noise signal need for filtration
  - sensitivity to droplets splashing onto the pressure sensor surface

- the necessity of using the optical technique for the determination of the time of contact between the fuel and the oxidiser
- low repeatability of results.

Based on the observed features of both techniques, the visual method shall be considered a better and more accurate option for ignition delay determination of hypergolic propellants. The optical method is sufficient to determine the ignition delay without any additional instrumentation. However, even in the visual determination of SOC, the pressure signal can be useful for triggering and data-collecting automation.

### Acknowledgements

The paper was prepared as a part of the HIPERGOL project, which is financially supported by the National Centre for Research and Development (NCBiR) under Grant No. DOB-BIO8/07/01/2016.



### Nomenclature

FTIR	Fourier-transform infrared
HTP	high-test peroxide
ID	ignition delay
IRFNA	inhibited red fuming nitric acid
MMH	monomethylhydrazine
NA	nitric acid

RFNA	red fuming nitric acid
RGHP	rocket grade hydrogen peroxide
SOC	start of combustion
TEAB	triethylamine borane
WFNA	white fuming nitric acid

### Bibliography

- [1] Ak MA, Ulas A, Sümer B, Yazici B, Yildirim C, Gönc LO et al. An experimental study on the hypergolic ignition of hydrogen peroxide and ethanalamine. *Fuel*. 2011;90(1):395-398. <https://doi.org/10.1016/j.fuel.2010.07.048>
- [2] Alfano AJ, Mills JD, Vaghjiani GL. Highly accurate ignition delay apparatus for hypergolic fuel research. *Rev Sci Instrum*. 2006;77(4). <https://doi.org/10.1063/1.2188909>
- [3] Blevins JJA, Gostowski R, Chianese S. An experimental investigation of hypergolic ignition delay of hydrogen peroxide with fuel mixtures. 42nd AIAA/ASME/SAE/ASEE Jt Propuls Conf Exhib. 2004;1335:1-8. <https://doi.org/10.2514/6.2004-1335>
- [4] Chambreau SD, Schneider S, Rosander M, Hawkins T, Gallegos CJ, Pastewait MF et al. Fourier transform infrared studies in hypergolic ignition of ionic liquids. *J Phys Chem A*. 2008;112(34):7816-7824. <https://doi.org/10.1021/jp8038175>
- [5] Chowdhury A, Wang S, Thynell S. Ignition behavior of novel hypergolic materials. 45th AIAA/ASME/SAE/ASEE Jt Propuls Conf Exhib. 2009:1-11. <https://doi.org/10.2514/6.2009-5352>
- [6] Chwist M. Comparative analysis of heat release in a reciprocating engine powered by a regular fuel with pyrolysis oil addition. *Combustion Engines*. 2022;190(3):104-12. <https://doi.org/10.19206/CE-146694>
- [7] Coil M. Hypergolic ignition of a gelled ionic liquid fuel. 46th AIAA/ASME/SAE/ASEE Jt Propuls Conf Exhib. 2010:1-11. <https://doi.org/10.2514/6.2010-6901>
- [8] Dambach E, Cho K, Pourpoint T, Heister S. Ignition of advanced hypergolic propellants. 46th AIAA/ASME/SAE/ASEE Jt Propuls Conf Exhib. 2010.
- [9] Davis SM, Yilmaz N. Advances in hypergolic propellants: ignition, hydrazine, and hydrogen peroxide research. *Adv Aerosp Eng*. 2014;2014(1):1-9. <https://doi.org/10.1155/2014/729313>
- [10] DeSain JD, Curtiss TJ, Metzler KM, Brady BB. Testing hypergolic ignition of paraffin wax/LiAlH<sub>4</sub> mixtures – AIAA 2010-6636. 46th AIAA/ASME/SAE/ASEE Jt Propuls Conf Exhib. 2010;1-19. <https://doi.org/doi:10.2514/6.2010-6636>
- [11] Gauthier BM, Davidson DF, Hanson RK. Shock tube determination of ignition delay times in full-blend and surrogate fuel mixtures. *Combust Flame*. 2004;139(4):300-311. <https://doi.org/10.1016/j.combustflame.2004.08.015>
- [12] Ghassemi H, Fasih HF. Application of small size cavitating venturi as flow controller and flow meter. *Flow Meas Instrum*. 2011;22(5):406-412. <https://doi.org/10.1016/j.flowmeasinst.2011.05.001>
- [13] Grochowalska J, Jaworski P, Kapusta ŁJ, Kowalski J. A new model of fuel spray shape at early stage of injection in a marine diesel engine. *Int J Numer Method H*. 2022;32(7):2345-2359. <https://doi.org/10.1108/HFF-05-2021-0349>
- [14] He Z, Yang J, Nie Z, Zhou X, Wu J. Preparation, characterization, and thermal decomposition kinetics of high test peroxide gel. *Acta Astronaut*. 2023;211:510-517. <https://doi.org/10.1016/j.actaastro.2023.07.001>
- [15] Heufer KA, Olivier H. Determination of ignition delay times of different hydrocarbons in a new high pressure shock tube. *Shock Waves*. 2010;20(4):307-316. <https://doi.org/10.1007/s00193-010-0262-2>
- [16] James MD, Kubal TD, Son SF, Anderson WE, Pourpoint TL. Calibration of an impinging jet injector suitable for liq-

- uid and gelled hypergolic propellants. 45th AIAA/ASME/SAE/ASEE Jt Propuls Conf Exhib. 2009:1-13. <https://doi.org/10.2514/6.2009-4882>
- [17] Jaworski A, Kuszewski H, Longwic R, Sander P. Assessment of self-ignition properties of canola oil–n-hexane blends in a constant volume combustion chamber and compression ignition engine. *Appl Sci*. 2023;13(19):10558. <https://doi.org/10.3390/app131910558>
- [18] Jyoti BVS, Naseem MS, Baek SW. Hypergolicity and ignition delay study of pure and energized ethanol gel fuel with hydrogen peroxide. *Combust Flame*. 2017;176:318-325. <https://doi.org/10.1016/j.combustflame.2016.11.018>
- [19] Kang H, Jang D, Kwon S. Demonstration of 500 N scale bipropellant thruster using non-toxic hypergolic fuel and hydrogen peroxide. *Aerosp Sci Technol*. 2016;49:209-214. <https://doi.org/10.1016/j.ast.2015.11.038>
- [20] Kang H, Lee E, Kwon S. Suppression of hard start for non-toxic hypergolic thruster using H<sub>2</sub>O<sub>2</sub> oxidizer. *J Propul Power*. 2017;33(5):1111-1117. <https://doi.org/10.2514/1.B36510>
- [21] Kapusta ŁJ, Boruc Ł, Kindracki J. Pressure and temperature effect on hypergolic ignition delay of triglyme-based fuel with hydrogen peroxide. *Fuel*. 2021;287:119370. <https://doi.org/10.1016/j.fuel.2020.119370>
- [22] Khomik SV, Usachev SV, Medvedev SP, Ivantsov AN, Stovbun SV, Mikhalkin VN et al. Reasonable testing of hypergolic fuels. *Acta Astronaut*. 2020;176:695-699. <https://doi.org/10.1016/j.actaastro.2020.02.053>
- [23] Li J, Fan W, Weng X, Tang C, Zhang X, Huang Z et al. Experimental observation of hypergolic ignition of superbase-derived ionic liquids. *J Propul Power*. 2018;34(1):125-132. <https://doi.org/10.2514/1.B36441>
- [24] Mahakali R, Kuipers FM, Yan AH, Anderson WE. Development of reduced toxicity hypergolic propellants. 47th AIAA/ASME/SAE/ASEE. Jt Propuls Conf Exhib. 2011:1-14. <https://doi.org/10.2514/6.2011-5631>
- [25] McCrary PD, Barber PS, Kelley SP, Rogers RD. Nonaborane and decaborane cluster anions can enhance the ignition delay in hypergolic ionic liquids and induce hypergolicity in molecular solvents. *Inorg Chem*. 2014;53(9):4770-4776. <https://doi.org/10.1021/ic500622f>
- [26] Merkisz J, Pielecha I, Łęgowik A. The assessment of autoignition of modified jet fuels. *Energies*. 2021;14(3):633. <https://doi.org/10.3390/en14030633>
- [27] Mota FAS, Fei L, Liu M, Jiang J, Tang C. Novel hypergolic green fuels with hydrogen peroxide for propulsion systems. *J Propul Power*. 2024;40(2):207-219. <https://doi.org/10.2514/1.B39224>
- [28] Mota FAS, Liu M, Mohsen AAA, Yao X, Mai Z, Tang C. Development of polyamine/alkanolamine-based hypergolics with hydrogen peroxide: a new route to n-methylimidazole with MDEA as a promising green fuel. *Fuel*. 2024;357:129798. <https://doi.org/10.1016/j.fuel.2023.129798>
- [29] Naber JD, Siebers DL, Di Julio SS, Westbrook CK. Effects of natural gas composition on ignition delay under diesel conditions. *Combust Flame*. 1994;99(2):192-200. [https://doi.org/10.1016/0010-2180\(94\)90122-8](https://doi.org/10.1016/0010-2180(94)90122-8)
- [30] Nath S, Mallick L, Lefkowitz JK. Hypergolic ignition response to oxidizer droplet properties. *Combust Flame*. 2023; 258:113061. <https://doi.org/10.1016/j.combustflame.2023.113061>
- [31] Park S, Lee K, Kang H, Park Y, Lee J. Effects of oxidizing additives on the physical properties and ignition performance of hydrogen peroxide-based hypergolic propellants. *Acta Astronaut*. 2022;200:48-55. <https://doi.org/10.1016/j.actaastro.2022.07.051>
- [32] Petersen EL, Kalitan DM, Barrett AB, Reehal SC, Mertens JD, Beerer DJ et al. New syngas/air ignition data at lower temperature and elevated pressure and comparison to current kinetics models. *Combust Flame*. 2007;149(1-2):244-247. <https://doi.org/10.1016/j.combustflame.2006.12.007>
- [33] Pourpoint T, Anderson W. Hypergolic reaction mechanisms of catalytically promoted fuels with rocket grade hydrogen peroxide. *Combust Sci Technol*. 2007;179(10):2107-2133. <https://doi.org/10.1080/00102200701386149>
- [34] Ramachandran PV, Kulkarni AS, Pfeil MA, Dennis JD, Willits JD, Heister SD et al. Amine-boranes: green hypergolic fuels with consistently low ignition delays. *Chem – Eur J*. 2014;20(51):16869-16872. <https://doi.org/10.1002/chem.201405224>
- [35] Szwaia M, Szymanek A. Combustion comparative analysis of pyrolysis oil and diesel fuel under constant-volume conditions. *Combustion Engines*. 2023;195(4):90-96. <https://doi.org/10.19206/CE-169805>
- [36] Türker L. Hypergolic systems based on hydrogen peroxide oxidizer. *Earthline J Chem Sci*. 2023;10(1):1-42. <https://doi.org/10.34198/ejcs.10123.142>
- [37] Wang SQ, Thynell ST. An experimental study on the hypergolic interaction between monomethylhydrazine and nitric acid. *Combust Flame*. 2012;159(1):438-447. <https://doi.org/10.1016/j.combustflame.2011.07.009>
- [38] Zarbo N, Belal H, Pourpoint TL. Effect of water and humidity on hypergolic propellant ignition delay. 51st AIAA/SAE/ASEE Jt Propuls Conf. 2015:1-15. <https://doi.org/10.2514/6.2015-3867>
- [39] Zhang Y, Shreeve JM. Dicyanoborate-based ionic liquids as hypergolic fluids. *Angew Chem Int Ed*. 2011;50(4):935-937. <https://doi.org/10.1002/anie.201005748>
- [40] Zhao X, Wang Z, Qi X, Song S, Huang S, Wang K et al. Hunting for energetic complexes as hypergolic promoters for green propellants using hydrogen peroxide as oxidizer. *Inorg Chem*. 2021;60(22):17033-17039. <https://doi.org/10.1021/acs.inorgchem.1c02149>

Łukasz Boruc, DEng. – Faculty of Power and Aeronautical Engineering, Warsaw University of Technology, Poland.  
e-mail: [Lukasz.Boruc@pw.edu.pl](mailto:Lukasz.Boruc@pw.edu.pl)



Łukasz Jan Kapusta, DEng. – Faculty of Power and Aeronautical Engineering, Warsaw University of Technology, Poland.  
e-mail: [Lukasz.Kapusta@pw.edu.pl](mailto:Lukasz.Kapusta@pw.edu.pl)



Jan Kindracki, DSc., DEng. – Faculty of Power and Aeronautical Engineering, Warsaw University of Technology, Poland.  
e-mail: [Jan.Kindracki@pw.edu.pl](mailto:Jan.Kindracki@pw.edu.pl)

